Heterogeneous Interaction of SO_2 on H_2O_2-Ice Films at 190−210 K

Liang Chu, Guowang Diao, and Liang T. Chu*

Department of Environmental Health and Toxicology, State University of New York at Albany, and Wadsworth Center, P.O. Box 509, Albany, New York 12201-0509

Received: April 6, 2000; In Final Form: June 9, 2000

Heterogeneous interaction of SO_2 on both the H_2O_2-ice surface and the water-ice surface has been investigated in a flow reactor interfaced with a differentially pumped quadrupole mass spectrometer. The initial uptake coefficient and uptake amount of SO_2 on the H_2O_2-ice surface and the water-ice surface were determined as a function of partial SO_2 pressures and ice film temperatures. The initial "true" uptake coefficient γ_o of SO_2 on 3% H_2O_2-ice surfaces is 3.2×10^{-4} and 8.3×10^{-5} at 192 and 211 K, respectively. The initial uptake coefficient γ_w of SO_2 on the water-ice film is 1×10^{-5} at 191 K. The uptake amount of SO_2 on the H_2O_2-ice surface at 192 K was determined in the range of 9.5×10^{12} to 5.3×10^{15} molecules/cm^2 as P_{SO_2} increased from 1.1×10^{-7} to 1.4×10^{-5} Torr, and the uptake amount of SO_2 on the water-ice surface at 191 K was 2.4×10^{12} molecules/cm^2 at $P_{SO_2} = 1.3 \times 10^{-6}$ Torr. The results suggested that the uptake of SO_2 on ice and snow surfaces was enhanced by the presence of H_2O_2 in ice at the temperature of the upper troposphere and lower stratosphere.

I. Introduction

Sulfur dioxide is an important gas in the atmosphere. The oxidation of sulfur dioxide to sulfuric acid in the atmosphere is of great interest because of the toxicity and deleterious environmental effects of sulfuric acid. Atmospheric sulfur dioxide can be removed by wet deposition and dry deposition.[1] For dry deposition to snow and aerosol, an understanding of the interaction of SO_2 on the ice surface is critical. Field measurements showed that the concentration of SO_4^{2-} in freshly fallen snow was larger than the concentration expected from particulate sulfate scavenging.[2,3] This result is closely related to the question of how gaseous SO_2 enters ice crystals by adsorption. It is essential to know how SO_2 interacts with the ice surface at the temperature of the upper troposphere and lower stratosphere. Previous studies also showed that the microphysical properties of cirrus clouds might have an important effect on the earth's climate and climatic feedback.[4] The uptake of SO_2, which is either from air or from jet exhaust, can reduce the vaporization rate of cirrus clouds and thus change the life expectancy of cirrus cloud particles. Subsequently, uptake of SO_2 impacts radiative forcing and climate.

The SO_2 concentration is about 50−100 ppt in the lower stratosphere, 50 ppt in the free troposphere, and 160 ppt in North America clean continental air.[1,5] SO_2 may be adsorbed on cloud particles, and adsorbed SO_2 is oxidized readily.[6] Several groups studied the SO_2 uptake on ice crystals.[7−10] These studies showed that the uptake of SO_2 reached a maximum at a temperature near 0 °C to −10 °C due to the presence of a quasi-liquid layer near the ice surface.[11,12] With decreasing temperature, the SO_2 uptake decreased.

H_2O_2 has been shown to oxidize S(IV) relatively rapidly in solution.[13−15] Husain and co-workers measured the oxidation of SO_2 by H_2O_2 with time in clouds at Whiteface Mountain in New York State.[16,17] H_2O_2 has been found in snowpacks worldwide.[18,19] Conklin et al. studied the uptake of SO_2 on H_2O_2-ice with varying bulk H_2O_2 composition (0−5 μM H_2O_2) at 213, 243, 265, and 272 K.[11] They reported the production of SO_4^{2-} as a function of H_2O_2 composition in the ice by melting the ice and then determining the SO_4^{2-} concentration. Results indicated that the $SO_2 + H_2O_2$ reaction can occur below 265 K (i.e., 243 and 213 K), and adsorbed SO_2 was irreversibly oxidized to SO_4^{2-}. However, they did not report the amount of SO_2 loss on the ice due to instability of the SO_2 detector. The production of SO_4^{2-} might be different from the SO_2 uptake. After SO_2 is adsorbed on the ice surface, one can speculate that SO_2 may exist as SO_2 molecules, or it may interact with water to form HSO_3^-, or it may further be oxidized to form SO_4^{2-}. To our best knowledge, there has been no direct measurement of the amount of SO_2 uptake reported in the literature. Both the uptake coefficient of SO_2 on ice and H_2O_2-ice, and the direct measurement of SO_2 uptake at low temperatures are unknown. This motivated us to study the interaction of SO_2 on water-ice and H_2O_2-treated ice surfaces at low temperatures.

In this paper, we report the first measurement of the uptake amount and uptake coefficient of SO_2 on the water-ice surface and H_2O_2-ice surface at 190−210 K. The uptake coefficient γ is defined as the ratio of the number of molecules that are taken up by the surface to the total number of molecules that collide on the surface. In the following sections, we will briefly describe the experimental procedures used in the determination of the uptake amount and the uptake coefficient. We will present the results of the uptake amount and uptake coefficient of SO_2 on the water-ice surface and the H_2O_2-ice surface as a function of ice film temperatures and partial pressures of SO_2.

II. Experimental Section

The measurements of the uptake amount and uptake coefficient of SO_2 on the H_2O_2-ice surface and on the water-ice surface were performed in a flow reactor coupled to a differ-

---

* To whom correspondence should be addressed. E-mail: lchu@csc.albany.edu.

10.1021/jp001323k CCC: \$19.00

entially pumped quadrupole mass spectrometer (QMS). Some of the apparatus details have been discussed in our previous publications,[20-22] and we provide only a brief description and some modifications in this paper.

Flow Reactor. The cylindrical flow reactor was constructed of Pyrex glass. Its dimensions were 1.70 cm inner diameter and 35 cm in length. The temperature of the reactor was regulated by a liquid nitrogen-cooled methanol circulator and was measured with a pair of J-type thermocouples located in the middle and at the downstream end. During the experiment, the temperature was maintained at 190− 211 K and the stability of the temperature was better than 0.3 °C in every experiment. The pressure of the reactor was controlled by a downstream throttle valve (MKS Instrument, model 651C), and the stability of the pressure was better than 0.001 Torr in every experiment.

Water-Ice and H_2O_2-Ice Film Preparation. Two types of ice films were prepared: the water-ice film and the H_2O_2-ice film. The water-ice film was prepared as follows: helium carrier gas (BOC, 99.9995%) was bubbled through a high purity distilled water (Millipore Milli-Q plus, $>18 M\Omega\cdot cm$) reservoir. The reservoir was maintained at 293.2 ± 0.1 K by a refrigerated circulator (Neslab, RTE-100LP). Helium saturated with water vapor was admitted to an inlet of the injector. The double capillary injector was slowly pulled out at a constant speed, 25 cm/min, and a uniform ice film was deposited on the inner surface of the reactor, which was at 190−211 K. The details have been discussed in our previous publications.[23,24]

The H_2O_2-ice film was prepared as follows: helium carrier gas was bubbled through an H_2O_2 solution (30 wt % or 3 wt % of H_2O_2, Aldrich). The helium flow rate was controlled by a mass flow controller (Teledyne). The solution was maintained at 273.2 K by a water−ice bath. Helium saturated with the H_2O_2 and water vapor was admitted to an inlet of the double capillary injector. The double capillary injector was slowly pulled out at a constant speed and a uniform H_2O_2-ice film was deposited on the inner surface of the reactor, which was at 190−211 K. The amount of H_2O_2-ice substrate deposited was determined from the mass flow rate of the H_2O_2 and water vapor mixture and the deposition time. The bulk composition of the H_2O_2-ice film was determined by a UV spectrometer after the H_2O_2-ice film was melted and collected. The H_2O_2-ice films were determined to contain 3.0 wt % of H_2O_2 and 0.8 wt % of H_2O_2 as prepared from the 30 wt % and 3 wt % H_2O_2 solution, respectively. The average film thickness was calculated using the measured ice film geometric area, the mass of H_2O_2 and H_2O vapor mixture, and the bulk ice density, 0.63 g/cm^3.[25] We assumed the bulk density of the H_2O_2-ice film was close to that of the water-ice since the H_2O_2-ice film contains only 0.8− 3.0 wt % of H_2O_2. The typical average film thickness was 2.4 ± 0.4 μm at 190 K, and 2.5 ± 0.3 μm at 211 K. After a uniform 17 cm ice film was deposited, an extra thick H_2O_2-ice film (~4 cm length) was deposited at the end of the flow tube in all experiments. The separation between the extra thick film and the uniform film was about 5 cm. Since the injector and helium carrier gases could be a few degrees warmer than the film, they would heat the extra ice film at the end of flow tube. This provided a source of both H_2O_2 and water vapor pressures in the flow tube to compensate for the loss of the film due to the pumping effect. This ensured the composition of H_2O_2-ice was about constant during the experiment.

Determination of the Concentration of H_2O_2. The concentration of the H_2O_2 solution was determined by a UV spectrometer (Beckman DU-600). Five standard H_2O_2 solutions, which contained 3.0, 2.0, 1.0, 0.5, and 0.25 wt % H_2O_2, were prepared from a 30 wt % H_2O_2 solution (Aldrich, 30 wt % ACS reagent). The standard H_2O_2 solutions were titrated by $KMnO_4$ solution, which was calibrated by an $H_2C_2O_4$ solution using a standard procedure. The UV absorption spectra of the five samples were measured and the molar absorption coefficient at 290 nm was determined to be 4.5 L mol^{-1} cm^{-1}. It was in excellent agreement with a literature value of $\epsilon = 4.6$ L mol^{-1} cm^{-1} at 290 nm.[26] To determine the composition of H_2O_2-ice films, the H_2O_2-ice film was melted and evacuated to a U-tube at liquid nitrogen temperature. The trapped H_2O_2-ice sample was then slowly warmed to room temperature. The sample was measured by UV spectrometry. Using the molar absorption coefficient at 290 nm, we determined that the H_2O_2-ice film prepared from the vapor of 30 wt % and 3 wt % H_2O_2 solutions was 3.0 wt % and 0.8 wt % of H_2O_2, respectively.

SO_2−He Mixtures. The SO_2−He mixture was prepared by mixing SO_2 (Linde, 99.98%) and helium (99.9995%) in an all-glass manifold, which had been previously evacuated to $\sim 10^{-6}$ Torr. SO_2 was a high purity commercial gas and was not further purified. The typical SO_2-to-He mixing ratio was 10^{-3} to 10^{-5}. SO_2 along with additional helium carrier gas, controlled by a Hasting−Teledyne mass flow controller, was introduced into the flow reactor via the glass and Teflon PFA tubing. All the tubings were passivated by the SO_2−He mixture to establish equilibrium as monitored by the QMS prior to every experiment. The amount of the SO_2−He mixture was controlled by two stainless needle valves in series, and its flow rate was determined from the pressure change in the manifold. The standard flow rate was calibrated in a separate experiment. Since the pressure of the manifold was about 400 Torr and the volume of the manifold is relatively large, the pressure change was only several Torr during the measurement. Therefore, the flow rate was constant during the experiment.

Determination of the Uptake Coefficient and Uptake Amount. The uptake coefficient of SO_2 on the H_2O_2-ice film and the water-ice film was determined in the following fashion: We use the SO_2 uptake on the H_2O_2-ice film to illustrate the procedures. First, an H_2O_2-ice film was vapor-deposited on the inner wall of the flow reactor. Second, SO_2, at a pressure between 5.4×10^{-8} and 1.5×10^{-5} Torr, was exposed to the H_2O_2-ice film surface. The gas-phase loss of SO_2 was measured by the QMS at $m/e^- = 64$ as a function of the injector distance z. For a first-order decay under plug-flow conditions, the following equation holds for SO_2:

$$\ln[SO_2]_z = -k_s(z/\upsilon) + \ln[SO_2]_0 \qquad (1)$$

where z is the injector position, υ is the flow velocity, $[SO_2]_z$ is the gas-phase SO_2 concentration measured by the QMS at position z, and sub-0 is the initial injector reference position. The first-order SO_2 decay for a typical experiment performed on the H_2O_2-ice film at 192 K is shown in Figure 1. The first-order loss rate constant, k_s, was calculated from the least-squares fit of the experimental data to eq 1. $k_s = 26.1$ s^{-1} at 192 K as shown in Figure 1. k_s was corrected for gas-phase axial and radial diffusion using a standard procedure,[27] and the corrected rate constant is called k_w. A diffusion coefficient (cm^2/s) for SO_2 in helium was used for the gas-phase diffusion correction and it was estimated using the Fuller equation.[28] This can be expressed as

$$D = (1.649 \times 10^{-2})T^{1.75}/P \qquad (2)$$

where T is the temperature in Kelvin and P is the total pressure

TABLE 1: Uptake Coefficient of SO_2 on the 3.0 wt % H_2O_2-Ice Surface at 192 K[a]

temperature (K)	P_{SO_2} (Torr)	v (m/s)	k_s (1/s)	k_w (1/s)	γ_w	γ_t
191.6 ± 0.1	5.4×10^{-8}	18.2	97 ± 29	103	$6.9 \pm 2.1 \times 10^{-3}$	$5.3 \pm 2.0 \times 10^{-4}$
191.5 ± 0.3	1.1×10^{-7}	17.9	53 ± 10	55	$3.7 \pm 0.8 \times 10^{-3}$	$2.4 \pm 0.6 \times 10^{-4}$
191.8 ± 0.1	1.7×10^{-7}	18.1	52 ± 13	56	$3.8 \pm 1.0 \times 10^{-3}$	$2.5 \pm 0.8 \times 10^{-4}$
191.7 ± 0.2	4.3×10^{-7}	17.8	30 ± 9	31	$2.1 \pm 0.6 \times 10^{-3}$	$1.3 \pm 0.4 \times 10^{-4}$
191.8 ± 0.1	5.8×10^{-7}	18.6	42 ± 18	43	$2.9 \pm 1.2 \times 10^{-3}$	$1.8 \pm 0.8 \times 10^{-4}$
192.0 ± 0.2	1.2×10^{-6}	19.3	29 ± 5	29	$2.1 \pm 0.4 \times 10^{-3}$	$1.3 \pm 0.3 \times 10^{-4}$
192.3 ± 0.3	1.6×10^{-6}	18.3	26 ± 5	27	$1.9 \pm 0.4 \times 10^{-3}$	$1.1 \pm 0.3 \times 10^{-4}$
191.7 ± 0.1	2.9×10^{-6}	18.0	27 ± 10	28	$1.8 \pm 0.9 \times 10^{-3}$	$1.1 \pm 0.6 \times 10^{-4}$
192.3 ± 0.1	7.5×10^{-6}	18.0	19 ± 4	19	$1.2 \pm 0.3 \times 10^{-3}$	$6.9 \pm 1.8 \times 10^{-5}$

[a] Total pressure was 0.500 ± 0.002 Torr; H_2O_2-ice film thickness was 2.4 ± 0.4 μm.

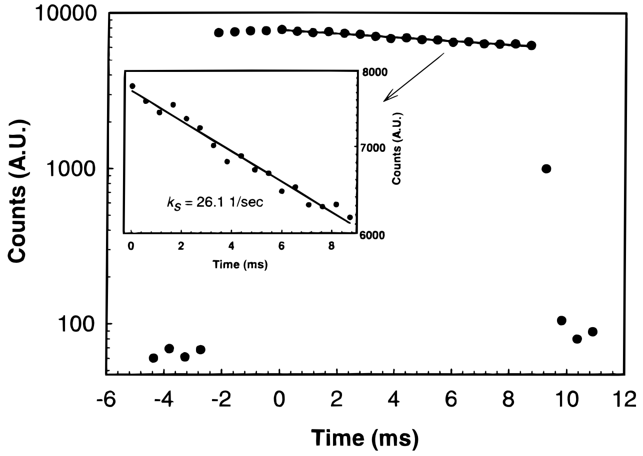

Figure 1. Plot of the SO_2 signal versus the reaction time (z/v) at 192 K. The plot shows the SO_2 background signal (< -2.5 ms), the initial signal before SO_2 was in contact with H_2O_2-ice ($t < 0$), and the loss of SO_2 on the film. The SO_2 flow was turned off at 8.5 ms after the reaction, and the signal was back to the background signal. The inserted plot shows the logarithm of SO_2 signal versus the reaction time. The pseudo first-order rate constant, k_s, = 26.1 s^{-1}, and the corrected rate constant, k_w, = 26.5 s^{-1}. The reaction probability, γ_w, = 7.3×10^{-4}. The total pressure = 0.501 Torr, and the flow velocity = 18.3 m/s.

of the reactor in Torr. The uptake coefficient γ_w was calculated from k_w using the following equation:[29]

$$\gamma_w = 2Rk_w/(\omega + Rk_w) \qquad (3)$$

where R is the radius of the flow reactor (0.85 cm) and ω is the mean SO_2 molecular velocity at the H_2O_2-ice film temperature. A layered pore diffusion model was employed to correct for ice surface roughness in order to obtain the "true" uptake coefficient γ_t.[29−31] γ_t reflected the uptake coefficient near the "top" surface area.

The uptake amount is defined as the total amount of SO_2 loss on the H_2O_2-ice surface. The SO_2−He mixture was flowed through the H_2O_2-ice surface till saturation. The loss of SO_2 onto the H_2O_2-ice surface was monitored by the QMS at $m/e^- = 64$. The measured SO_2 signal was proportional to the concentration of SO_2 admitted into the flow tube. The uptake amount can be determined from the total gaseous SO_2 loss to the surface. The detailed procedure can be found from our previous work.[20,32]

III. Results

Uptake Coefficients of SO_2 on H_2O_2-Ice Films. The uptake coefficient of SO_2 on the H_2O_2-ice film was determined by observing the decay of gaseous SO_2, monitored by the QMS, as a function of injection position. In every measurement, the H_2O_2-ice film was freshly prepared. The measured γ_w represents the initial uptake coefficient. Two different kinds of H_2O_2-ice film were prepared, which contained 3.0 wt % of H_2O_2 and 0.8 wt % H_2O_2, respectively.

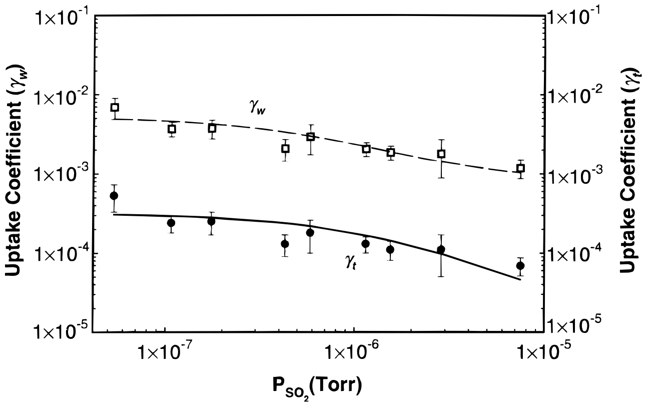

Figure 2. Plot of the initial uptake coefficient γ_w (☐) and γ_t (●) versus the partial SO_2 pressures for SO_2 uptake on 3.0 wt % H_2O_2-ice surfaces at 191.8 K. The H_2O_2-ice film thickness was 2.4 ± 0.4 μm. The dashed line was an empirical fit and the solid line was a fit of the experiment data γ_t to the model with $\gamma_o = 3.2 \times 10^{-4}$ and $b = 8 \times 10^5$. See text for details.

Uptake Coefficient of SO_2 on 3.0 wt % H_2O_2-Ice Films. The initial uptake coefficient γ_w was determined at 191.8 ± 0.3 K. The mean values of γ_w, γ_t, temperatures, and experimental conditions are tabulated in Table 1. The measured first-order rate constant, k_s, was averaged from 2 to 5 measurements, and the error bar represents one standard deviation of the mean value. The "true" uptake coefficient γ_t was obtained by using a layered pore diffusion model for the ice surface roughness correction. On the basis of previous studies, which were conducted at similar conditions,[30,31,33] H_2O-ice films can be approximated as hexagonally close-packed spherical granules stacked in layers.[31] The "true" uptake coefficient, γ_t, is related to the value, γ_w, by

$$\gamma_t = \frac{\sqrt{3}\gamma_w}{\pi\{1 + \eta[2(N_L - 1) + (3/2)^{1/2}]\}} \qquad (4)$$

where N_L is the number of granule layers and η is the effectiveness factor.[34] η is a function of the tortuosity factor τ and true ice density ρ_t. $\tau = 4$ and $\rho_t = 0.925$ g/cm^3 were used in the above calculation.[31,35] This was based on a treatment of the ice film vapor-deposited on the flow tube, and we adapted these values as the best approximation.

The initial uptake coefficient γ_w of SO_2 on 3.0 wt % H_2O_2-ice films as a function of the SO_2 partial pressures at 192 K is also presented in Figure 2. Figure 2 shows that γ_w was decreased slightly from 6.9×10^{-3} to 1.2×10^{-3} when the SO_2 partial pressure increased from 5.4×10^{-8} to 7.5×10^{-6} Torr. The dashed line was a fit to the experimental data and used to guide the eye only. γ_t showed a similar trend.

TABLE 2: Uptake Coefficient of SO_2 on the 3.0 wt % H_2O_2-Ice Surface at 211 K[a]

temperature (K)	P_{SO_2} (Torr)	v (m/s)	k_s (1/s)	k_w (1/s)	γ_w	γ_t
210.8 ± 0.2	5.3×10^{-7}	19.7	24 ± 4	24	$1.5 \pm 0.3 \times 10^{-3}$	$8.7 \pm 1.9 \times 10^{-5}$
211.4 ± 0.3	8.4×10^{-7}	19.2	18 ± 5	18	$1.2 \pm 0.4 \times 10^{-3}$	$6.9 \pm 2.4 \times 10^{-5}$
211.8 ± 0.2	1.5×10^{-6}	19.8	26 ± 9	26	$1.7 \pm 0.5 \times 10^{-3}$	$1.0 \pm 0.3 \times 10^{-4}$
211.0 ± 0.2	2.3×10^{-6}	18.8	17 ± 6	17	$1.1 \pm 0.4 \times 10^{-3}$	$6.3 \pm 2.4 \times 10^{-5}$
211.4 ± 0.1	3.2×10^{-6}	18.7	17 ± 6	17	$1.1 \pm 0.4 \times 10^{-3}$	$6.3 \pm 2.4 \times 10^{-5}$
210.8 ± 0.2	5.0×10^{-6}	19.2	25 ± 11	26	$1.8 \pm 0.8 \times 10^{-3}$	$1.1 \pm 0.5 \times 10^{-4}$
211.4 ± 0.3	1.1×10^{-5}	19.5	22 ± 3	23	$1.5 \pm 0.2 \times 10^{-3}$	$8.7 \pm 1.2 \times 10^{-5}$
211.0 ± 0.3	1.5×10^{-5}	20.0	23 ± 3	24	$1.5 \pm 0.2 \times 10^{-3}$	$8.7 \pm 1.2 \times 10^{-5}$

[a] Total pressure was 0.500 ± 0.002 Torr; H_2O_2-ice film thickness was 2.5 ± 0.2μm.

TABLE 3: Uptake Coefficient of SO_2 on the 0.8 wt % H_2O_2-Ice Surface at 191 K[a]

temperature (K)	P_{SO_2} (Torr)	v (m/s)	k_s (1/s)	k_w (1/s)	γ_w	γ_t
190.3 ± 0.2	2.5×10^{-7}	17.5	9 ± 4	9	$6.0 \pm 3.0 \times 10^{-4}$	$3.3 \pm 1.7 \times 10^{-5}$
190.4 ± 0.4	5.0×10^{-7}	17.8	27 ± 13	28	$1.8 \pm 0.9 \times 10^{-3}$	$1.1 \pm 0.6 \times 10^{-4}$
190.6 ± 0.2	7.1×10^{-7}	17.8	6 ± 3	6	$3.9 \pm 1.9 \times 10^{-4}$	$2.1 \pm 1.1 \times 10^{-5}$
190.0 ± 0.1	1.0×10^{-6}	18.0	11 ± 4	11	$7.6 \pm 2.7 \times 10^{-4}$	$4.2 \pm 1.6 \times 10^{-5}$
190.6 ± 0.2	1.5×10^{-6}	18.1	25 ± 16	25	$1.7 \pm 1.1 \times 10^{-3}$	$1.0 \pm 0.7 \times 10^{-4}$
189.4 ± 0.3	2.3×10^{-6}	18.6	6 ± 3	6	$4.4 \pm 2.2 \times 10^{-4}$	$2.4 \pm 1.2 \times 10^{-5}$
191.8 ± 0.2	5.8×10^{-6}	17.3	5 ± 2	6	$3.7 \pm 1.6 \times 10^{-4}$	$2.0 \pm 0.9 \times 10^{-5}$
191.7 ± 0.1	3.1×10^{-5}	9.8	3 ± 1	3	$2.1 \pm 1.0 \times 10^{-4}$	$1.1 \pm 0.5 \times 10^{-5}$

[a] Total pressure was 0.500 ± 0.002 Torr; H_2O_2-ice film thickness was 2.4 ± 0.3 μm.

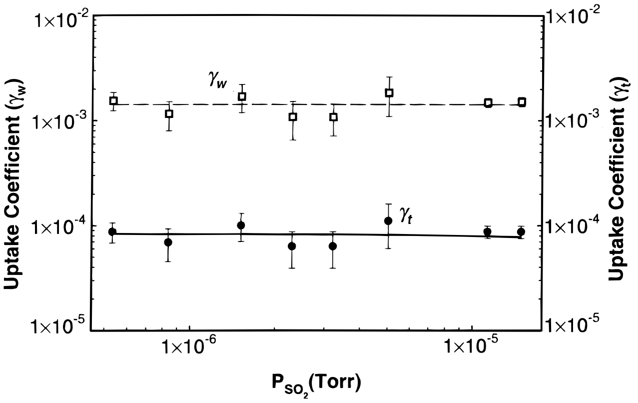

Figure 3. Plot of the initial uptake coefficient γ_w (□) and γ_t (●) versus the partial SO_2 pressures for SO_2 uptake on the H_2O_2-ice surface at 211.2 K. The H_2O_2-ice film thickness was 2.5 ± 0.1 μm, and H_2O_2 composition was 3.0 wt %. The solid line is a fit of the experimental data γ_t to the model and results in an initial "true" uptake coefficient of $(8.3 \pm 0.7) \times 10^{-5}$.

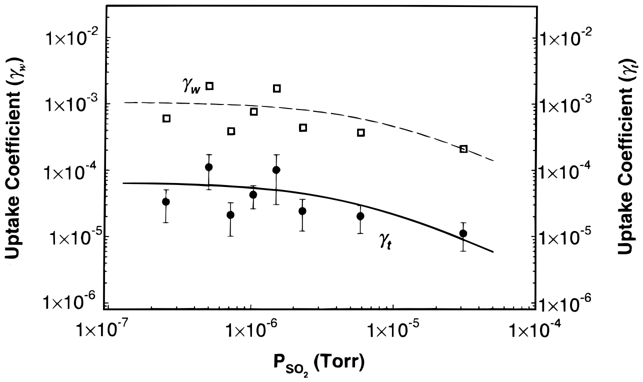

Figure 4. Plot of the uptake coefficient γ_w (□) and γ_t (●) versus the partial SO_2 pressures for SO_2 uptake on the H_2O_2-ice surface at 190.6 K. The H_2O_2-ice film thickness was 2.4 ± 0.3 μm, and the composition of H_2O_2 was 0.8 wt %. The solid line was a least-squares fit of γ_t data to the model with $\gamma_o = 6.4 \times 10^{-5}$ and $b = 2 \times 10^5$ and the dashed line was used to guide the eye. See text for details.

The measurements were also conducted at a warmer temperature, 211.2 ± 0.4 K. The mean values of γ_w and γ_t for SO_2 on 3.0 wt % H_2O_2-ice film at 211 K are tabulated in Table 2. Again, the included errors represent one standard deviation of the mean value. Figure 3 is a plot of γ_w and γ_t versus the SO_2 partial pressures at 211 K. The uptake coefficient γ_w of SO_2 on the 3.0 wt % H_2O_2-ice film at 211 K was in the range of 1.1×10^{-3} to 1.8×10^{-3} as the SO_2 partial pressure changed from 5.3×10^{-7} to 1.5×10^{-5} Torr. The γ_w values were nearly a constant as SO_2 partial pressure increased. The solid line was a fit to the experimental data γ_t as discussed in a later section. In general, the initial uptake coefficients of SO_2 on the 3.0 wt % H_2O_2-ice film at 211 K were lower than at 192 K.

Uptake Coefficient of SO_2 on 0.8 wt % H_2O_2-Ice Films. The H_2O_2-ice film that contained 0.8 wt % of H_2O_2 was prepared by depositing the vapor of 3 wt % H_2O_2 solutions onto the cooled glass wall surface. The initial uptake coefficients of SO_2 on 0.8 wt % H_2O_2-ice films at 190.6 ± 0.8 K and experimental conditions are tabulated in Table 3 and presented in Figure 4. The errors bars in Table 3 and Figure 4 are one standard deviation of the mean value. The dashed line in Figure 4 was an empirical fit to γ_w, and the solid line was a least-squares fit of γ_t to the model that will be discussed. Figure 4 shows that the γ_w values were decreased from 1.8×10^{-3} to 2.1×10^{-4} when the SO_2 partial pressure increased from 2.5×10^{-7} to 3.1×10^{-5} Torr. The uptake coefficient of SO_2 on 0.8 wt % H_2O_2-ice films was lower than that on 3.0 wt % H_2O_2-ice films as indicated in Figures 2 and 4. However, they showed a similar trend, i.e., the γ_w values decreased as the SO_2 partial pressure increased.

Uptake of SO_2 on the H_2O_2-Ice Film. *Surface Density as a Function of Temperature*. The uptake amount of SO_2 on 3.0 wt % H_2O_2-ice films at 191−213 K is presented in Figure 5. The uptake amount Θ was expressed as a surface density. It decreased from 4.7×10^{15} to 7.1×10^{13} molecules/cm^2 when the temperature increased from 191 to 213 K at $P_{SO_2} = 1.3 \times 10^{-6}$ Torr. The "heat of uptake" of SO_2 on the 3.0 wt % H_2O_2-ice surface was calculated from the slope of a plot of ln Θ versus $1/T$.[36,20] The heat of uptake ΔH was determined to be −6 ± 4 kcal/mol. This indicates that uptake is an exothermal process.

Surface Density as a Function of Partial SO_2 Pressure. Figure 6 shows the uptake amount Θ of SO_2 on 3.0 wt % H_2O_2-ice films at 192 K as a function of the SO_2 partial pressures. The uptake amount was increased from 5.9×10^{12} to 7.0×10^{15}

TABLE 4: Uptake Coefficient of SO_2 on the Pure Ice Surface at 191 K[a]

temperature (K)	P_{SO_2} (Torr)	v (m/s)	k_s (1/s)	k_w (1/s)	γ_w	γ_t
191.0 ± 0.3	7.2×10^{-6}	2.1	0.14 ± 0.05	0.14	$1.2 \pm 0.4 \times 10^{-5}$	$5.4 \pm 1.8 \times 10^{-7}$
190.8 ± 0.2	9.2×10^{-6}	4.7	0.11 ± 0.04	0.11	$8.1 \pm 0.3 \times 10^{-6}$	$3.7 \pm 0.1 \times 10^{-7}$
190.8 ± 0.2	1.2×10^{-5}	2.1	0.18 ± 0.06	0.18	$1.4 \pm 0.3 \times 10^{-5}$	$6.3 \pm 1.4 \times 10^{-7}$
192.2 ± 0.5	1.5×10^{-5}	2.2	0.23 ± 0.07	0.23	$1.5 \pm 0.4 \times 10^{-5}$	$6.7 \pm 1.8 \times 10^{-7}$
192.0 ± 0.4	1.9×10^{-5}	2.1	0.45 ± 0.14	0.45	$3.0 \pm 1.5 \times 10^{-5}$	$1.4 \pm 0.7 \times 10^{-6}$
190.8 ± 0.2	2.3×10^{-5}	4.8	0.17 ± 0.06	0.17	$1.3 \pm 0.6 \times 10^{-5}$	$5.9 \pm 2.7 \times 10^{-7}$

[a] Total pressure was 2.000 ± 0.002 Torr; H_2O-ice film thickness was 3.1 ± 0.3 μm.

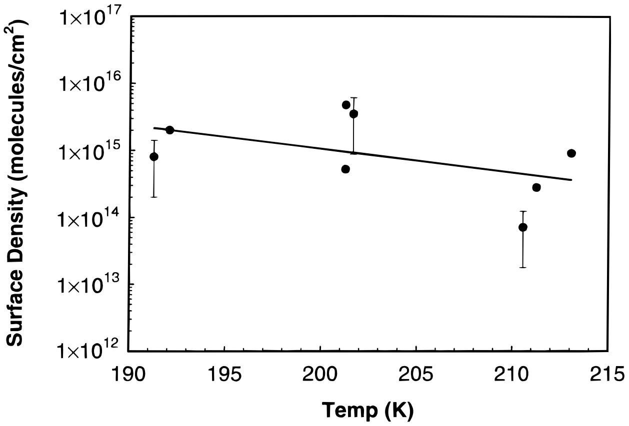

Figure 5. Plot of the surface density of SO_2 on the H_2O_2-ice surface versus the H_2O_2-ice film temperature. H_2O_2-ice film thickness was 2.5 ± 0.3 μm, and the film contained 3.0 wt % of H_2O_2. $P_{SO_2} = 1.3 \times 10^{-6}$ Torr. A typical error of measurement is shown in the . The solid line is the least-squares fit of the experiment data.

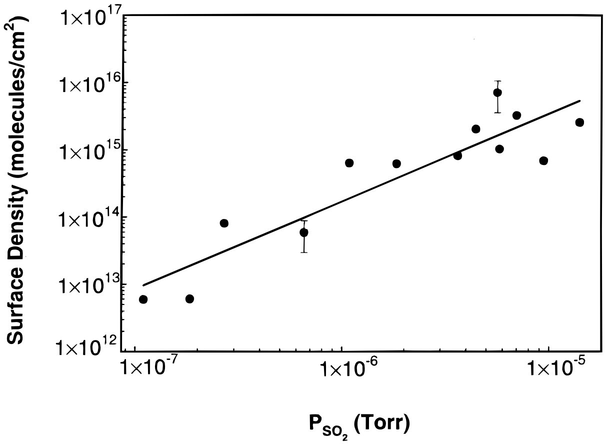

Figure 6. Plot of the surface density of SO_2 on the H_2O_2-ice surface versus the partial SO_2 pressures at 191.8 K. The H_2O_2-ice film thickness was 2.5 ± 0.4 μm, and the film contained 3.0 wt % of H_2O_2.

molecules/cm^2 as the partial pressure of SO_2 increased from 1.1×10^{-7} to 1.4×10^{-5} Torr. The solid line was fitted to $\Theta = KP^n$, where $K = 1.1 \times 10^{22}$ when P is in Torr and Θ is in molecules cm^{-2}, and $n = 1.3$.

Uptake of SO_2 on the Water-Ice Film. *Uptake Coefficient of SO_2 on Water-Ice.* The initial uptake coefficients of SO_2 on water-ice films at 191.3 ± 0.6 K and experimental conditions are tabulated in Table 4 and presented in Figure 7. Within a narrow partial SO_2 pressure range (7.2×10^{-6} to 2.3×10^{-5} Torr), the values of γ_w fluctuated slightly from 8.1×10^{-6} to 3.0×10^{-5}. Within experimental uncertainty, γ_w is nearly independent of partial SO_2 pressure under our experiment conditions.

Surface Density of SO_2 on the Water-Ice Film. Figure 8 is a plot of the SO_2 signal versus the experimental time for exposure of SO_2 on a water-ice surface. In this experiment, a 26 cm length of the ice film was deposited on the wall of the flow reactor. The gas-phase SO_2 signal, as monitored by the QMS at $m/e^- = 64$, decreased when SO_2 reached the entire ice surface. The entire ice film was saturated in less than 30 s at 191 K. The small SO_2 signal loss reflected a lower γ_w value. The uptake amount was determined to be about 2.4×10^{12} molecules/cm^2 at 191 K.

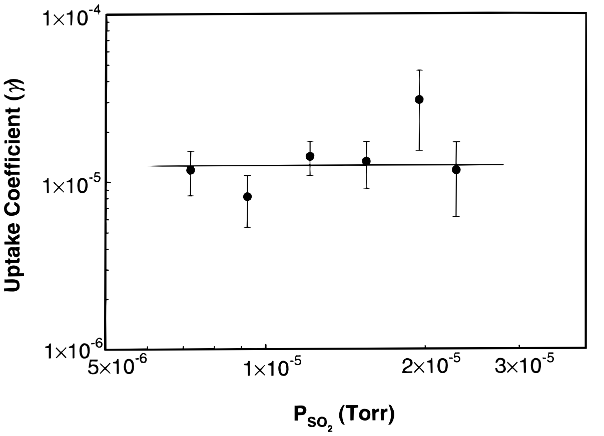

Figure 7. Plot of the uptake coefficient γ_w versus partial SO_2 pressures for SO_2 uptake on the water-ice surface at 191.3 K. The ice film thickness was 3.1 ± 0.3 μm. The solid line is a mean value of the experiment data.

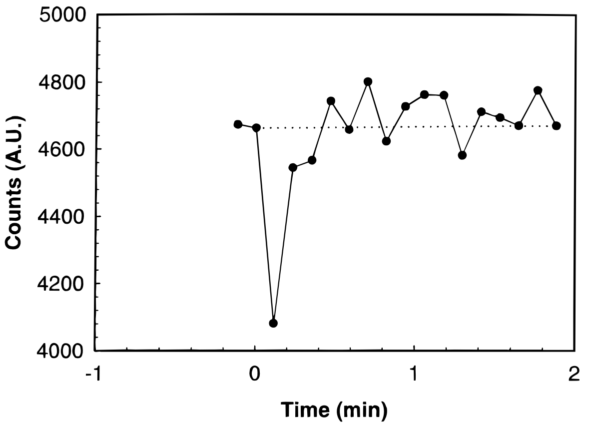

Figure 8. Plot of the SO_2 signal versus the experimental time for SO_2 uptake on a water-ice surface at 190.9 K. The ice film thickness was 3.0 μm. The partial SO_2 pressure was 1.3×10^{-6} Torr. The uptake amount of SO_2 on pure water-ice was 2.4×10^{12} molecules/cm^2.

IV. Discussion

Uptake of SO_2 on the Water-Ice Film versus on the H_2O_2-Ice Film. The experimental results indicated that initial uptake coefficients of SO_2 on the water-ice surface at 191 K were in the range of 1×10^{-5} (see Figure 7), which is about 100-fold lower than γ_w on the H_2O_2-ice film (1.2×10^{-3} to 6.9×10^{-3}, Figure 2). The uptake amount of SO_2 on the water-ice film at 191 K was 2.4×10^{12} molecules/cm^2, and the uptake amount of SO_2 on the H_2O_2-ice film at 192 K was in the range of 9.5×10^{12} to 5.3×10^{15} molecules/cm^2. It is clear that the chemical nature of the SO_2 uptake on water-ice films is different from that on H_2O_2-ice films. On the basis of SO_2 oxidation in the aqueous phase and $SO_2-H_2O_2$ aqueous chemistry,[1] it is reasonable to ask whether SO_2 is oxidized on the H_2O_2-ice film to form SO_4^{2-}. In a separate experiment, after SO_2 was taken up by the H_2O_2-ice film, we collected products, including the H_2O_2-ice film, in a U-tube at liquid-nitrogen temperature. The collected sample was then warmed to room temperature. The sample was analyzed by ion-exchange chromatography (IC) (Dionex, DX 500, IonPac AS 14 column) for SO_4^{2-} and other components. The IC was calibrated with a K_2SO_4 (AR, Aldrich) solution. The standard deviation of measurements for this analysis was better than 10%.[37] A known concentration (2.899 mM) sulfuric acid solution was used to test the IC method. The uncertainty of this analysis was indeed within 10%. We determined the formation of SO_4^{2-} from the SO_2 in the H_2O_2-ice sample. However the amount of sulfate was equivalent to about 50% of the SO_2 uptake amount. There are two possible uncertainties: (i) SO_4^{2-} or H_2SO_4 might remain on the glass wall during the collection because of its low vapor pressure. The vapor pressure of pure H_2SO_4 at 293 K is about 7×10^{-5} Torr,[38] so the partial H_2SO_4 pressure over the sulfuric acid solution at 273 K should be lower than 10^{-5} Torr. The sample was vacuum transferred from the flow reactor to the U-tube by a mechanical pump; it is possible that a fraction of H_2SO_4 may have remained on the glass surface due to its low vapor pressure. Experimentally, we were not able to achieve a higher vacuum because the flow reactor was constructed of glass and sealed by Viton O-rings. Also, there was a movable injector in the reactor. The ultimate vacuum limit is 10^{-4} to 10^{-5} Torr. (ii) Another issue is whether SO_2 is completely converted to sulfate near the surface. One may speculate that SO_2 molecules taken up by H_2O_2-ice may exist in part as bisulfite ion (HSO_3^-). However, the rate constant k_o for the reaction of $HSO_3^- + H_2O_2$ in aqueous solutions is in the range of 1×10^2 L mol^{-1} s^{-1} at pH = 5−6 and 298 K.[39] The reaction half-life $t_{1/2}$ was 0.01 s, provided there was a sufficient amount of H_2O_2 near the surface (see later discussion). If HSO_3^- formed near the surface, HSO_3^- should be converted to sulfate rapidly. This is provided that the oxidation rate is as efficient as at 298 K. It certainly possible that this pathway is decreased by orders of magnitude at 191 K and only part of HSO_3^- was oxidized to SO_4^{2-}. Unfortunately, with our current experiment setup, we cannot directly measure the formation of HSO_3^- on the surface, if any. It is important to point out that, if it was HSO_3^- near the surface, the mass balance for sulfur should be satisfied. The conclusion of this discussion is that SO_2 is predominantly oxidized to SO_4^{2-} near the H_2O_2-ice surface at 191 K, and some sulfate may remain in the reactor because it does not completely transfer out for analysis.

Desorption Temperature of H_2O_2 on Ice. The gas-phase oxidation of SO_2 by H_2O_2 is expected to be extremely slow,[39] even the rate constant for $HO_2 + SO_2$ reaction was 1×10^{-18} cm^3 molecules^{-1} s^{-1} at 298 K.[40] Under fast flow-tube conditions, the gas-phase oxidation of SO_2 by H_2O_2 is an insignificant process. The question we are asking is whether H_2O_2 remained on the surface and was available for the reaction during the entire experiment. We need to know the temperature at which H_2O_2 leaves the surface under our experimental conditions.

The desorption temperature of H_2O_2 on the ice surface was determined using the temperature-programmed desorption technique. After the 3.0 wt % H_2O_2-ice film was deposited on the wall of the flow reactor at 190 K, we ramped the temperature of the flow reactor at ∼3 K/min and monitored both the gas-phase H_2O_2 and water molecules by QMS. Both gas-phase H_2O_2 and water vapor signals versus the temperature are presented in Figure 9. The desorption temperature of H_2O_2 on the ice surface was about 218 K, and was 215 K for water. The film was erupted above 215 K. This implies that H_2O_2 was both adsorbed on the surface and in the film in our experimental conditions when the temperature was lower than 215 K.

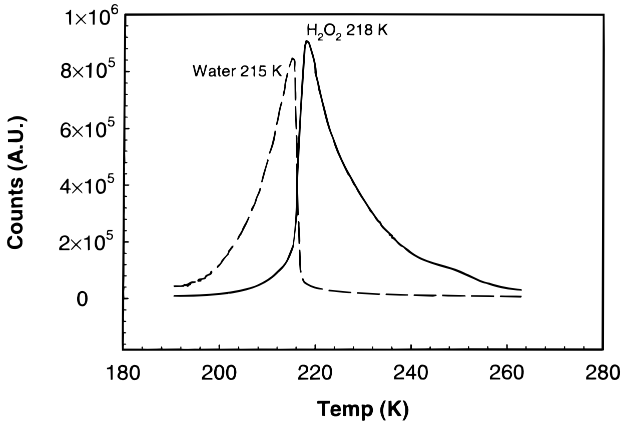

Figure 9. A thermal desorption spectrum of a 3 wt % H_2O_2-ice film. The thickness of the film was 2.6 μm. The desorption temperature for H_2O_2 (solid line) was 218 K. The dashed line shows the water signal. Its desorption temperature was 215 K at a total pressure of 0.5 Torr.

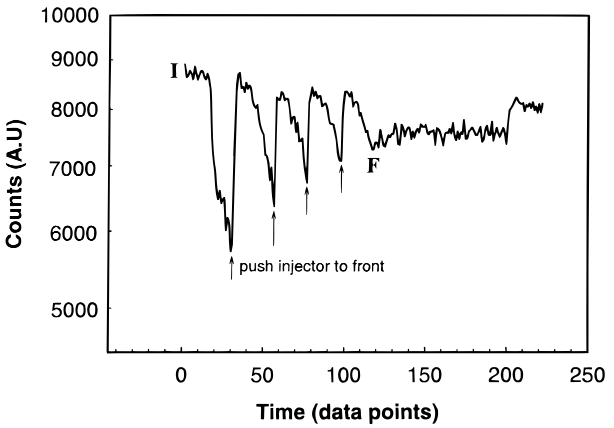

Figure 10. Plot of the SO_2 signal versus the reaction time at 189.6 K. After an initial SO_2 uptake on a freshly prepared H_2O_2-ice (first arrow), the injector was pushed back to the front and the measurement was repeated. The uptake coefficient of SO_2 on the H_2O_2-ice surface was measured up to an additional four times on the same surface, as indicated by arrows. The initial uptake coefficient γ_w of SO_2 was 1.2 $\times 10^{-3}$. The second to fifth uptake coefficients of SO_2 were 7.9×10^{-4}, 5.8×10^{-4}, 4.9×10^{-4}, and 3.7×10^{-4}, respectively. The H_2O_2-ice film thickness was 2.4 μm.

Effect of the Partial SO_2 Pressure and Temperature on the Uptake Coefficient. *Effect of Partial SO_2 Pressures on H_2O_2-Ice Surfaces.* Figures 2 and 4 show that the initial uptake coefficient γ_w or γ_t decreased as the partial SO_2 pressure increased at 191 K. Also, additional measurements, shown in Figure 10, indicate that the uptake coefficients decrease as the successive exposure SO_2 to the surface increases. These appear to show surface saturation effects. The behavior of SO_2 on the H_2O_2-ice surface can be described as follows. After an H_2O_2-ice surface is exposed to gaseous SO_2, a fraction of surface θ is covered by SO_2 and the remaining “clean” H_2O_2-ice surface is $1 - \theta$.[41,42] We assume that the H_2O_2 surface concentration was a constant during the uptake and the change of its concentration was ignored. The process is represented by the following reactions:

$$SO_2(g) + H_2O_2(surf) \underset{k_d}{\overset{k_{ad}}{\rightleftharpoons}} SO_2\text{---}H_2O_2(ad) \xrightarrow{k_r} \text{Product} \quad (5)$$

and the gas-phase SO_2 loss rate can be expressed by

$$-\frac{d[SO_2(g)]}{dt} = [k_{ad}[SO_2(g)](1-\theta) - k_d\theta[SO_2(ad)]_0]\frac{S}{V} \quad (6)$$

where $[SO_2(g)]$ is the SO_2 volume concentration, $[SO_2(ad)]_0$ is a monolayer SO_2 concentration, and S/V is the surface-to-volume ratio. Apply the steady-state approximation to $[SO_2(ad)]$, i.e., $d(\theta[SO_2(ad)]_0)/dt = 0$ and solve θ, eq 6 can be simplified to

$$-\frac{d[SO_2(g)]}{dt} = \frac{k_{ad}k_r[SO_2(g)][SO_2(ad)]_0}{(k_d + k_r)[SO_2(ad)]_0 + k_{ad}[SO_2(g)]}\frac{S}{V} \quad (7)$$

The uptake coefficient can be expressed as

$$\gamma_t = \frac{-\dfrac{d[SO_2(g)]}{dt}}{\dfrac{S}{4V}[SO_2(g)]\omega} = \frac{k_r[SO_2(ad)]_0}{(k_d + k_r)[SO_2(ad)]_0 + k_{ad}[SO_2(g)]} \quad (8)$$

where ω is the thermal velocity of SO_2, $k_{ad} = \alpha\omega/4$ where α is the accommodation coefficient, and the $[SO_2(g)]$ concentration can be written in terms of partial pressure of SO_2, $P_{SO_2,}$ and temperature T. Equation 8 can be rewritten as

$$\gamma_t = \frac{k_r[SO_2(ad)]_0/\alpha}{(k_d + k_r)[SO_2(ad)]_0 + \dfrac{k_{ad}}{k_B T}P_{SO_2}} \quad (9)$$

where k_B is the Boltzmann constant. At constant temperature, eq 9 becomes

$$\gamma_t = \frac{\gamma_o}{(1 + bP_{SO_2})} \quad (10)$$

where $\gamma_o = k_r/(k_d + k_r)\alpha$ and $b = k_{ad}/((k_d + k_r)[SO_2(ad)]_0 k_B T)$. The parameter γ_o represents the initial "true" uptake coefficient as the partial pressure of SO_2 approaches zero, in which the surface saturation effect is vanished.

The experimental data, γ_t, were fitted to eq 10 and they are shown in Figures 2−4 as the solid line. The fitted curve represents the experimental results very well. This suggests that model works well under the current experimental conditions. The parameter, γ_o, was determined to be $3.2 \pm 0.5 \times 10^{-4}$ and $6.4 \pm 1.7 \times 10^{-5}$ at 191 K for 3% H_2O_2-ice and 0.8% H_2O_2-ice surfaces, respectively. γ_o value is very close to measured "true" uptake coefficients at low pressures ($P_{SO_2} \leq 10^{-7}$ Torr). Note, the above treatment compounded H_2O_2 surface concentrations into the uptake coefficient. The ratio of the γ_o value for two different H_2O_2-ice surfaces is 5. The ratio is close to the bulk H_2O_2 concentration ratio 3.8 (= 3/0.8). The γ_o value is equivalent to the initial "true" uptake coefficient on a given H_2O_2-ice surface concentration.

The Effect of Temperatures on the Uptake Coefficient. The initial uptake coefficient decreased as the H_2O_2-ice film temperature increased from 192 to 211 K as shown in Figures 2 and 3. γ_w values at 211 K are nearly independent of the partial SO_2 pressure changes. These observations can be qualitatively explained by the above model. At 211 K, k_d is about 5−10-fold higher than that at 192 K on the basis of $k_d = \upsilon_d \exp(-\Delta E_{ad}/RT)$ where ΔE_{ad} is the heat of adsorption. It is approximately equal to heat of uptake determined to be −6 kcal/mol. $k_{ad} = \alpha\omega/4$ and ω is proportional to the square root of T. Thus, the effect of the temperature on k_{ad} is about 5% and can be ignored in our discussion. This means both the γ_o and b parameter in eq 10 are smaller at 211 K. Thus, γ_w or γ_t is lower at 211 K and γ_t is insensitive to P_{SO_2} as bP_{SO_2} is smaller.

It is expected that the surface and bulk H_2O_2 diffusion−exchange rate is higher at 211 K. This was ignored in the above simple treatment. The net result is to maintain a nearly constant supply of H_2O_2 on the surface. In another word, the variation of the "clean" surface $(1 - \theta)$ with the SO_2 coverage is also reduced at a higher temperature.

Effect of the Partial SO_2 Pressures on the Water-Ice Surface. Both uptake coefficient and uptake amount are small at 191 K and there are no observed surface saturation effects within the experimental uncertainty. The initial uptake coefficient can be modeled by the precursor model.[43] This is illustrated by the following reactions.

$$SO_2(g) \underset{k_{-1}}{\overset{k_1}{\rightleftharpoons}} SO_2\ (\text{precursor}) \xrightarrow{k_2} SO_2(ad) \quad (11)$$

The loss rate of gaseous SO_2 is given by

$$-\frac{d[SO_2(g)]}{dt} = \{k_1[SO_2(g)] - k_{-1}[SO_2(pre)]\}\frac{S}{V} \quad (12)$$

The precursor $SO_2(pre)$ concentration can be determined using the steady-state approximation $-d[SO_2(pre)]/dt = 0$, and eq 12 can be rewritten as

$$-\frac{d[SO_2(g)]}{dt} = \frac{k_1k_2}{k_{-1} + k_2}[SO_2(g)]\frac{S}{V} \quad (13)$$

The uptake coefficient can be expressed as

$$\gamma = \frac{-\dfrac{d[SO_2(g)]}{dt}}{\dfrac{[SO_2(g)]\omega S}{4V}} = \frac{4k_1k_2}{\omega(k_{-1} + k_2)} \quad (14)$$

Equation 14 indicated that the initial uptake coefficient of SO_2 on the water-ice surface at constant temperature is independent of the partial pressure of SO_2. This is in excellent agreement with the experimental results as shown in Figure 7.

Estimation of the H_2O_2 Surface Concentration. Do H_2O_2-ice surfaces have enough H_2O_2 molecules to react with SO_2? We can approximately estimate the surface concentration of H_2O_2. Two H_2O_2-ice films, 0.8 wt % and 3.0 wt % of H_2O_2-ice films, were used in this study. We assumed the bulk density of the H_2O_2-ice is similar to that of pure ice, 0.63 g/cm^3.[29] There are (total) 2.1×10^{22} molecules/cm^3. Each molecule occupies approximately 4.8×10^{-23} cm^3. We assume all molecules are closely packed together and the size of each molecule is approximately 3.6×10^{-8} cm. This is equivalent to having the surface area of each molecule be 1.3×10^{-15} cm^2. That is 7.6×10^{14} molecules per square centimeter. For the 3.0 wt % of H_2O_2-ice film, the molecular ratio of H_2O_2 to H_2O is 16:1000. Assuming H_2O_2 molecules are homogeneously distributed in the film, the surface density of H_2O_2 is 1.2×10^{13} molecules/cm^2. For the typical 2.4 μm H_2O_2-ice films, there are about 6700 layers of molecules. However, the surface concentration of H_2O_2

is usually higher than its bulk.[43] If all H_2O_2 molecules were at the surface, the surface concentration would be 8.0×10^{16} molecules/cm^2. This is an unrealistic upper limit of the surface concentration of H_2O_2. The "true" surface concentration of H_2O_2 on the H_2O_2-ice surface would be somewhere between 1.2×10^{13} and 8.0×10^{16} molecules/cm^2 and, of course, it should be closer to the lower end.

Let us examine how many H_2O_2 molecules would be used during an uptake coefficient measurement, if $P_{SO_2} = 1 \times 10^{-6}$ Torr. The flux of SO_2 was $^1/_4 n\omega\gamma(S/V)$, where n is the number of gaseous SO_2 molecules per cubic centimeter, which is 5×10^{10} molecules/cm^3 at 192 K. ω is about 2.5×10^4 cm/s. γ is the uptake coefficient of SO_2 on the H_2O_2-ice surface. The exposure time of SO_2 on the H_2O_2-ice surface was 10 s for each measurement. The flux of SO_2 was about 2.5×10^{12} molecules/cm^2 for $\gamma = 10^{-3}$. The flux of SO_2 was lower than the surface concentration of H_2O_2 ($>1.2 \times 10^{13}$ molecules/cm^2). The conclusion of this discussion is that the surface concentration of H_2O_2 is sufficient for reacting with SO_2 on 3.0 wt % H_2O_2-ice surface.

Figure 10 shows that, after SO_2 was exposed to the H_2O_2-ice surface for a total of five times, the H_2O_2 surface was not completely saturated by SO_2 as witnessed by the SO_2 signal (after a mark F in Figure 10). Clearly, SO_2 was still taken up by the surface after the last measurement. This supports the above discussion which indicated the surface concentration of H_2O_2 is sufficient for reactions.

Atmospheric Application. We should use our experimental data to compare the relative efficiency of SO_2 loss on the snow versus in the aerosol in the atmosphere. The typical H_2O_2 concentration in the atmosphere is 1 ppb, and tropospheric snow/ice always contains a trace amount of H_2O_2. On the basis of this study, the uptake coefficient of SO_2 on snow would be approximately 10^{-5}, and γ of SO_2 on 0.8 wt % H_2O_2-ice surface is 10^{-3} at 191 K. At a warmer temperature (250 K), γ is expected to be lower. We will use $\gamma = 10^{-5}$ in this discussion. The loss rate of 1 ppb SO_2 on the ground snow/ice is calculated to be 4×10^9 molecules cm^{-2} s^{-1} by using eq 15 below

$$-\frac{d[SO_2(g)]}{dt} = \frac{1}{4} n\omega\gamma_w \qquad (15)$$

The loss rate of SO_2 in the aerosol (aqueous phase) in the atmosphere is estimated to be 8×10^7 molecules cm^{-3} s^{-1} by using $R_a = 581$ (% h^{-1}) with aerosol density of 0.4 g/m^2 at 273 K.[1] The γ of SO_2 loss on the aerosol can be converted to 1.8×10^{-4} using a reaction rate constant of 1×10^2 M^{-1} s^{-1} and Henry's law constant $H = 1.23$ M atm^{-1}.[39,44] For these two processes, the uptake coefficients are comparable. The loss rate of SO_2 per unit area of snow is larger than that in an aerosol per unit volume of air. This indicates that the SO_2 loss on snow is an important sink in a cold area in winter. Earlier field studies have shown that sulfates are scavenged more efficiently by snow than by winter rain.[45,46] A modeling study showed that 27% of SO_2 was removed from atmosphere by dry deposition, mainly by snow and ice.[47] These data are in agreement with our estimates. If we take the snow-condensed phase mixing ratio into account, the amount of SO_2 loss on the snow/ice aerosol should be substantially decreased. This would be the case for SO_2 loss to cirrus clouds. Comprehensive atmospheric chemistry modeling is required to assess the effect.

Comparison. There are no identical measurements of SO_2 uptake on ice reported previously. We may make comparisons to some relevant studies. Conklin et al.[11] reported the production of SO_4^{2-} was 2.0×10^{-7} g/m^2 for SO_2 on deionized water-ice, and 1.6×10^{-6} g/m^2 for SO_2 on 0.5 μM H_2O_2-ice at 213 K. This is equivalent to 1.3×10^{13} molecules/cm^2 and 9.9×10^{13} molecules/cm^2 in terms of the SO_2 surface concentration, respectively. Our measurement result was 2.4×10^{12} molecules/cm^2 on water-ice and 9.5×10^{12} to 5.3×10^{15} molecules/cm^2 on 3.0 wt % H_2O_2-ice film at 192 K. Our results were slightly different from those of Conklin et al. because of the difference in temperature and H_2O_2 concentrations. Abbatt and co-workers are studying the uptake of SO_2 on ice, and their results are in agreement with this work.[48]

Worsnop et al. studied SO_2 uptake on water droplets, and Jayne et al. measured the uptake coefficient on 1 M H_2O_2 (3.1 wt %) droplets.[15,49] The uptake coefficient of SO_2 on water droplets at pH = 7 was 0.11 at 273 K and was decreased to ~0.005 at pH = 3. The uptake coefficient of SO_2 on 1 M H_2O_2 droplets at pH = 3 was ~0.03 at 283 K and was strongly depending on the pH. The SO_2 uptake efficiency is enhanced slightly in the H_2O_2 droplet. Their results showed that SO_2 was efficiently taken up by water droplets at warmer temperatures (273−283 K). However, SO_2 is not easily taken up on the ice surface and H_2O_2 does enhance the SO_2 uptake on the ice surface at lower temperature (190 K), according to this study.

V. Conclusion

This study shows that the initial uptake coefficient γ_w of SO_2 on water-ice at 191 K is in the range of 1×10^{-5} and the uptake amount of SO_2 on water-ice at 191 K was 2.4×10^{12} molecules/cm^2. The initial "true" uptake coefficient γ_o of SO_2 on 3.0 wt % and 0.8% H_2O_2-ice films at 191 K is $(3.2 \pm 0.5) \times 10^{-4}$ and $(6.4 \pm 1.7) \times 10^{-5}$, respectively. $\gamma_o = (8.3 \pm 0.7) \times 10^{-5}$ is lower at a higher temperature 211 K. The uptake amount of SO_2 on 3.0 wt % H_2O_2-ice films at 192 K varied with the SO_2 partial pressure. The uptake of SO_2 on ice was enhanced by the presence of H_2O_2 on the ice surface and SO_2 was oxidized to sulfate.

Acknowledgment. The authors thank Drs. L. Husain, V. A. Dutkiewicz, and O. Rattigan for helpful discussions. The authors also acknowledge the assistance by Dr. C. Judd, A. R. Khan, and S. Qureshi for the calibration of hydrogen peroxide and the measurement of sulfate, and the use of a UV spectrometer at the Biochemistry Core facility. This work was supported by the National Science Foundation under Grant ATM-9530659.

References and Notes

(1) Seinfeld, J. H.; Pandis, S. N. *Atmospheric Chemistry and Physics*; Wiley: New York, 1998; Chapters 6 and 19.
(2) Colin, J. L.; Renard, D.; Lescoat, V.; Jaffrezo, J. L.; Gros, J. M.; Strauss, B. *Atmos. Environ.* **1989**, *23*, 1487.
(3) Tranter, M.; Brimblecombe, P.; Davies, T. D.; Vincent, C. E.; Abvehams, P. W.; Blackwood, I. *Atmos. Environ.* **1986**, *20*, 517.
(4) Stephens, G. L.; Tsay, S. C.; Stackhouse, P. W.; Flatau, P. J. *J. Atmos. Sci.* **1990**, *47*, 1742.
(5) Stolarski, R. S.; Wesoky, H. L. *The Atmospheric Effects of Stratospheric Aircraft: A Third Program Report*; NASA Reference Publication 1313, NASA Office of Space Science and Applications, Washington, DC, November 1993; pp 267−271.
(6) Valdez, M. P.; Bales, R. C.; Stanley, D. A.; Dawson, G. A. *J. Geophys. Res.* **1987**, *92*, 9779.
(7) Choi, J.; Conklin, M. H.; Bales, R. C.; Sommerfeld, R. A. *Atmos. Environ.* **2000**, *34*, 793.
(8) Diehl, K.; Mitra, S. K.; Pruppacher, H. R. *Atmos. Res.* **1998**, *47−48*, 235.
(9) Mitra, S. K.; Barth, S.; Pruppacher, H. R. *Atmos. Environ.* **1990**, *24A*, 2307.
(10) Sommerfeld, R. A.; Lamb, D. *Geophys. Res. Lett.* **1986**, *13*, 349.
(11) Conklin, M. H.; Sommerfeld, R. A.; Laird, S. K.; Villinski, J. E. *Atmos. Environ.* **1993**, *27A*, 159.
(12) Conklin, M. H.; Bales, R. C. *J. Geophys. Res.* **1993**, *98*, 16851.

(13) Hoffmann, M. R.; Edwards, J. O. *J. Phys. Chem.* **1975**, *79*, 2096.

(14) Penkett, S. A.; Jones, B. M. R.; Bruice, K. A.; Eggleton, A. E. J. *Atmos. Environ.* **1979**, *13*, 123.

(15) Worsnop, D. R.; Zahniser, M. S.; Kolb, C. E.; Gardner, J. A.; Watson, L. R.; Van Doren, J. M.; Jayne, J. T.; Davidovits, P. *J. Phys. Chem.* **1989**, *93*, 1159.

(16) Husain, L.; Dutkiewicz, V. A.; Husain, M. M.; Khwaja, H. A.; Burkhard, E. G.; Mehmood, G.; Parekh, P. P.; Canelli, E. *J. Geophys. Res.* **1991**, *96*, 18789.

(17) Husain, L.; Dutkiewicz, V. A. *J. Geophys. Res.* **1992**, *97*, 14635.

(18) Neftel, A.; Jacob, P.; Klockow, D. *Nature* **1984**, *311*, 43.

(19) Gunz, D. W.; Hoffmann, M. R. *Atmos. Environ.* **1990**, *24A*, 1661.

(20) Chu, L. T.; Heron, J. W. *Geophys. Res. Lett.* **1995**, *22*, 3211.

(21) Chu, L. T. *J. Vac. Sci. Technol. A* **1997**, *1*5, 201.

(22) Chu, L.; Chu, L. T. *J. Phys. Chem. A* **1999**, *103*, 691.

(23) Chu, L.; Chu, L. T. *J. Phys. Chem. A* **1999**, *103*, 8640.

(24) Chu, L.; Diao, G.; Chu, L. T. *J. Phys. Chem. A* **2000**, *104*, 3150.

(25) Keyser, L. F.; Leu, M.-T. *J. Colloid Interface Sci.* **1993**, *155*, 137.

(26) Taylor, R. C.; Cross, P. C. *J. Am. Chem. Soc.* **1949**, *71*, 2266.

(27) Brown, R. L. *J. Res. Natl. Bur. Stand. (U.S.)* **1978**, *83,* 1.

(28) Cussler, E. L. *Diffusion, mass transfer in fluid systems*; Cambridge University Press: New York, 1984; Chapter 4.

(29) Chu, L. T.; Leu, M.-T.; Keyser, L. F. *J. Phys. Chem.* **1993**, *97*, 12798.

(30) Keyser, L. F.; Moore, S. B.; Leu, M.-T. *J. Phys. Chem.* **1991**, *95*, 5496.

(31) Keyser, L. F.; Leu, M.-T.; Moore, S. B. *J. Phys. Chem.* **1993**, *97*, 2800.

(32) Chu, L. T.; Chu, L. *J. Phys. Chem. B* **1997**, *101*, 6271.

(33) Keyser, L. F.; Leu, M.-T. *Microsc. Res. Tech.* **1993**, *25*, 343.

(34) The parameter N_L can be found in refs 23, 24, and 31. Also see ref 31 for detailed calculation procedures.

(35) Chu, L. T.; Leu, M.-T.; Keyser, L. F. *J. Phys. Chem.* **1993**, *97*, 7779.

(36) Abbatt, J. P. D.; Molina, M. J. *Geophys. Res. Lett.* **1992**, *19*, 461.

(37) Khwaja, H. A.; Khan, A. R.; Qureshi, S. *Intern. J. Environ. Anal. Chem.* **1999**, *75* (3), 285.

(38) Lide, D. R. *CRC Handbook of Chemistry and Physics*, 78th ed.; CRC Press: New York, 1998; p 8.44.

(39) Finlayson-Pitts, B. J.; Pitts, J. N., Jr. *Atmospheric Chemistry*; Wiley: New York, 1986; Chapter 11.

(40) Atkinson, R.; Baulch, D. L.; Cox, R. A.; Hampson, R. F., Jr.; Kerr, J. A.; Troe, J *J. Phys. Chem. Ref. Data* **1992**, *21*, 1125.

(41) Boudart, M.; Djéga-Mariadassou, G. *Kinetics of Heterogeneous Catalytic Reactions*; Princeton University Press: Princeton, 1984; pp 44−56.

(42) Gershenzon, M. Y.; Il'In, S.; Fedotov, N. G.; Gershenzon, Y. M.; Aparina, E. V.; Zelenov, V. V. *J. Atmos. Chem.* **1999**, *34*, 119.

(43) Masel, R. I. *Principles of Adsorption and Reaction on Solid Surfaces*; Wiley: New York, 1996; Chapter 5.

(44) Kolb, C. E.; Worsnop, D. R.; Zahniser, M. S.; Davidovits, P.; Keyser, L. F.; Leu, M.-T.; Molina, M. J.; Hanson, D. R.; Ravishankara, A. R.; Williams, L. R.; Tolbert, M. A. In *Progress and Problems in the Atmospheric Chemistry*; Barker, J. R., Ed.; World Scientific: River Edge, NJ, 1995; Chapter 18.

(45) Chan, W. H.; Chung, D. H. S. *Atmos. Environ.* **1986**, *20*, 1397.

(46) Dasch, J. M. *Atmos. Environ.* **1987**, *21*, 137.

(47) Wojcik, G. S.; Chang, J. S. *J. Atmos. Chem.* **1997**, *26*, 109.

(48) Abbatt, J. P. D. Personal communication.

(49) Jayne, J. T.; Gardner, J. A.; Davidovits, P.; Worsnop, D. R.; Zahniser, M. S.; Kolb, C. E. *J. Geophys. Res.* **1990**, *95*, 20559.